

RESEARCH PAPER

Diverse Nano Dimension of SDS, PEG and CTAB Roofed MgO Nano Powder Synthesized by Co-precipitation Method

Rajendran Varadharajan and Deepa Baskaran*

PG Research Department of Physics, Presidency College, Chennai, Tamilnadu, India

ARTICLE INFO

Article History:

Received 24 April 2017

Accepted 2 June 2017

Published 01 July 2017

Keywords:

Crystal structure

FTIR

Nanoparticles

ABSTRACT

The SDS, PEG and CTAB roofed MgO nano powders were synthesized by co-precipitation method. The sintered nano powders was shown Fm-3m space group with cubic phase obtained by the XRD pattern. The lattice strain was calculated to be used Williamson-Hall equations (W-H). The formation of Mg-O bond and hydroxyl radicals on the surface were confirmed by the FTIR analyses. The TEM revealed that the morphology of sintered nano powders has three different dimensions (0D, 1D, 2D) with average crystallites size was about ~20-80 nm and length usually 200-500 nm. The UV-DRS spectra show that the ionic surfactants roofed MgO leads to band gap shrinkage. The evaluated optical band gap energy is $E_g = 4.10\text{eV}$, 3.41eV and 3.12eV for SDS, PEG and CTAB-MgO nano powder respectively. Also extending light absorption towards the visible region due to decrease in crystallite size of surfactants roofed MgO nano powders utilizing for photocatalytic purpose and opto electronic devices.

How to cite this article

Varadharajan R, Baskaran D. Diverse Nano Dimension of SDS, PEG and CTAB Roofed MgO Nano Powder Synthesized by Co-precipitation Method. J Nanostruct, 2017; 7(3):189-193. DOI: 10.22052/jns.2017.03.004

INTRODUCTION

The insulating oxide, MgO having wide band gap ($>6\text{ eV}$) and even surface features have been selected for importunate opto-electronic applications [1-3]. Significantly, MgO can be used for reactive adsorbents, they used to the cleansing of chemical warfare agents [4], dropping chlorofluorocarbons [5] and humanizing the transesterification reaction at the supercritical/subcritical temperatures [6]. Considerable concern is focused on the control of the size and morphology of nanocrystalline materials can lead to the discovery of new physical and chemical properties [7]. Desirably, small particles are roofed by different organic molecules, which form a chemical bond with the molecules on the particle surface. Such materials are considered to have potential applications in biological cell dissolution, in magnetic separation of minerals, as fillers in polymer matrices, and also for the removal of toxic

* Corresponding Author Email: b.deepasenthil@gmail.com

elements from industrial wastes [8]. However, large scale, high-efficiency controlled synthesis of nanostructures still remains as a challenge. In that, co-precipitation method is capable way to synthesis of nano size particles due to its simple course, high yielding and enthralling method. In this work, we successfully synthesize MgO nanopowder by co-precipitation method using magnesium acetate hexahydrate and phthalic acid with three different ionic surfactants. The morphological, structural and optical properties of the SDS, PEG, and CTAB roofed MgO nano powders are reported.

MATERIALS AND METHODS

1.5 g of magnesium acetate hexahydrate [$\text{Mg}(\text{CH}_3\text{COO})_2$] was dissolved in 50 ml of double distilled water and kept was under stirring. 0.8 g of phthalic acid was added to the above solution. After that, 1 g of sodium dodecyl sulfate (SDS) was added into the solution; the white sol was stirred

for few hours then dried at 100°C for entire day. The above procedure was repeated for PEG and CTAB roofed samples in spite of SDS. Then, dried sample was washed systematically to eliminate the impurities. The yield SDS, PEG and CTAB roofed MgO precipitate resin dried ambient temperature and then sintered at 600° for 360 min in alumina crucible.

Characterization Techniques

The as synthesized samples were systematically characterized using various techniques. The X-ray diffraction (XRD) patterns of the MgO were obtained by the XRD Analytical X’Pert Pro MPD with CuKα radiation. The morphology and size of the MgO crystallites were determined using a scanning electron microscope (SEM; JEOL JSM-7600 F,) and a High resolution transmission electron microscope (HRTEM; JEOL JEM-2100 F). UV-Vis spectrum of the sample was recorded on Perkin Elmer- Lambda Spectrometers in the range of 190-1100 nm.

RESULT AND DISCUSSION

The X-ray diffraction pattern of cationic, anionic and non-ionic surfactant assisted MgO nano powder was shown in Fig. 1(a). The XRD pattern revealed that the nano powder have an Fm-3m space group with cubic phase. The finer orientation plane and diffracting angle of cubic nano powder is (200) at 2θ= 42.89775°, 42.84443°, 42.8542°. The other peaks at 2θ values of 36.6525°, 62.2756°, 74.6436°, 78.6036°: 36.8541°, 62.2344°, 74.6328°, 78.5807° and 36.8689°, 62.2489°, 74.6114°, 78.5781° are respectively to correspond (111), (220), (311) and (222) orientation planes of SDS, PEG and CTAB-MgO nano powder.. The observed

diffraction pattern was consistent with standard JCPDS file (04-0829). Small peaks are observed in the diffraction pattern of SDS- MgO at an angle 20-35°. This may be due to the sulfate in SDS. No extra contamination peaks were observed in the other diffraction patterns revealed that prepared nano powders are of high purity and crystalline in nature. The crystallite size of surfactants assisted MgO were calculated by the Debye-Scherrer equation [9]

$$D = k\lambda/\beta\cos\theta \tag{1}$$

where D – average crystallite size, K – shape factor (0.94), λ – wavelength of Cu Kα radiation (1.541 Å), β – Full Width Half Maximum (FWHM) of reflection (in radians) located at 2θ and θ –angle of reflection (in degrees) was used to relate the crystallite size to the line broadening. The average crystallite size was found to be about 33.75 nm, 20.27 nm and 18.70 nm for SDS, PEG and CTAB-MgO respectively.

The induced strain in powders due to crystal defect and deformation was calculated using the formula:

$$\varepsilon = \beta_{hkl}/4 \tan\theta \tag{2}$$

From Equations 1 and 2, it was confirmed that the peak width from crystallite size varies as 1/cosθ strain varies as tanθ. Assuming that the particle size and strain contributions to line broadening are independent to each other and both have a Cauchy-like profile, the observed line breadth is simply the sum of Equations 1 and 2 and rearranging the above equation, we get

$$\beta_{hkl} \cos\theta = k\lambda/D + 4\varepsilon \sin\theta \tag{3}$$

The above equations are Williamson-Hall

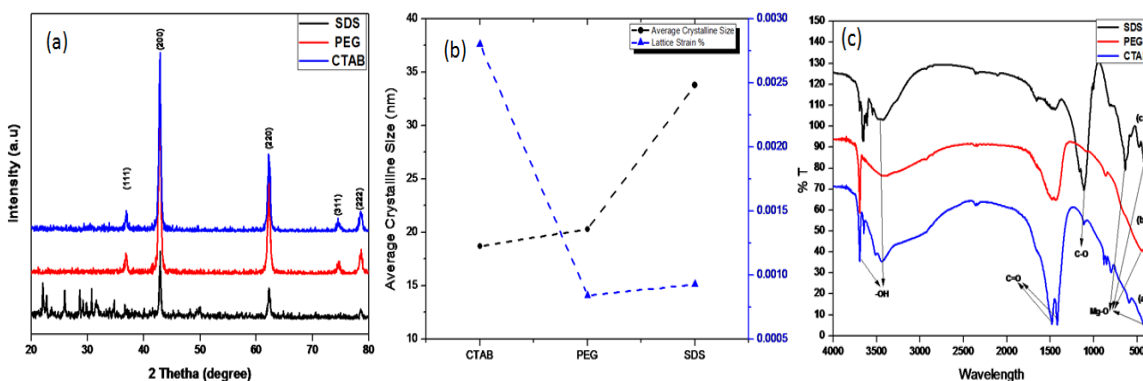


Fig.1. SDS, PEG and CTAB roofed MgO of (a) XRD pattern, (b) Graph of Crystalline size with Lattice Strain and (c) FTIR Spectra.

equations. A plot is drawn with $4\sin\theta$ along the x-axis and $\beta_{hkl} \cos\theta$ along the y-axis for as-prepared MgO nano powders. From the linear fit to the data, the crystalline size was estimated from the y-intercept, and the strain ϵ , from the slope of the fit. The strain was assumed to be uniform in all crystallographic directions, thus considering the isotropic nature of the crystal, where the material properties are independent of the direction along which they are measured [10].

The room temperature FT-IR spectrum of (a) CTAB, (b) PEG, (c) SDS- MgO shown in Fig.1 (c). Spectra (a), (b) and (c) observed the sharp feature band at $\sim 3650\text{-}3695\text{ cm}^{-1}$ and the wide stretching band at 3442 cm^{-1} indicates the formation of hydroxyl group (-OH) on the crystal face [11] and intensity weakened due to the distribution of hydroxyl group on the MgO surface. The major widened peak in the IR range $400\text{-}600\text{ cm}^{-1}$ which is the ascribed the formation of Mg-O bonds [12]. At spectra SDS-MgO, that peak should be splitted into two bands indicate that the low frequency

stretching band (ν_2) [9]. The absorption band at $2360, 2366$ and 2362 cm^{-1} may absorb CO_2 in air [13]. In CTAB-MgO spectra shows the asymmetric stretching vibration of carbonate ion at 1483.26 and 1421.54 cm^{-1} (ν_3 mode) indicating the existence of carbonate as bicarbonate species [11]. In SDS-MgO spectra observed the spiky peak at 1112.93 and 1163.08 cm^{-1} is related to the proportion of saturated acyl group, which is close agreement with the reported values [14]. The above studies established the formation and purity of the MgO nano powder.

The SEM images of SDS, PEG and CTAB-MgO nano powders shows petite crystallites of consistent allocation and their shapes is not clearly discernable due to the tiny crystallites which is requires higher resolution capability. The TEM images of synthesized nano powder visibly shown in Fig.2 revealed that the nano powder has different morphologies and the ionic surfactants roofed around the nano particle surface. The morphologies of CTAB have 2D- hexagonal with

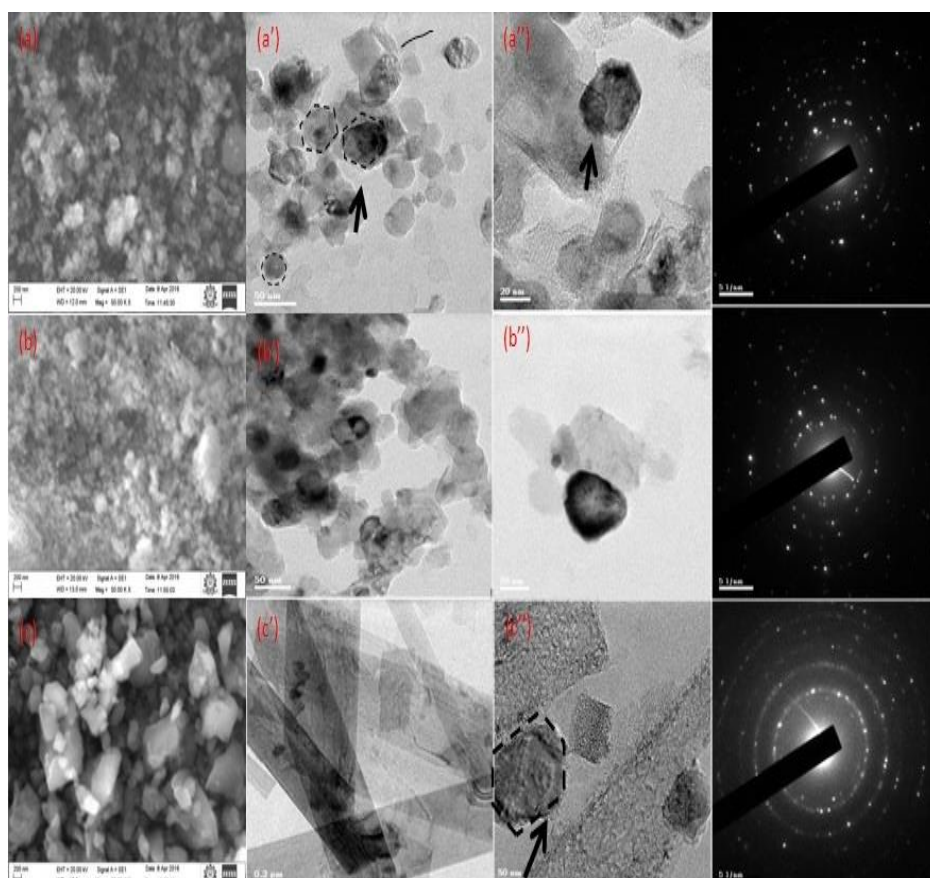


Fig. 2. (a), (b) and (c) SEM images, (a'), (b') and (c') TEM images (a''), (b'') and (c'') HR-TEM images and simultaneous SAED pattern of CTAB, PEG and SDS - MgO nano powders.

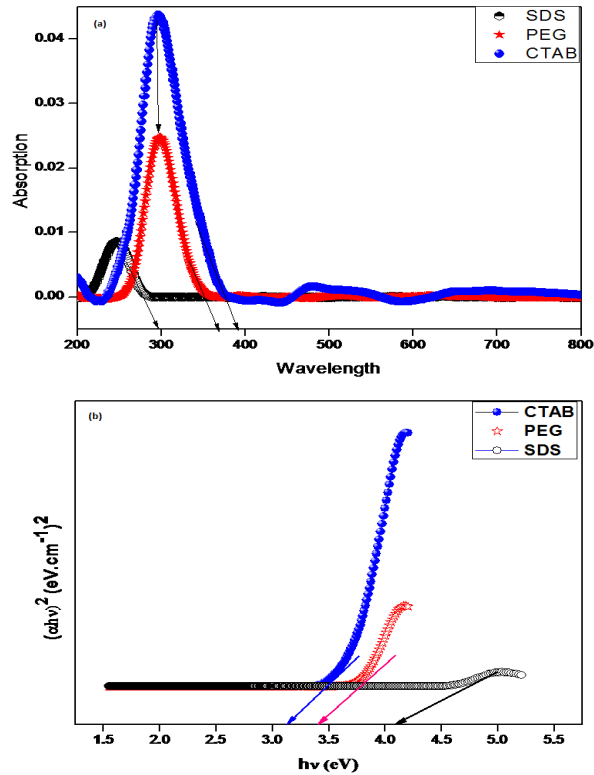


Fig. 3. (a) UV-DRS Spectra, (b) corresponding Tauc's plot of SDS, PEG and CTAB- MgO nano powder.

few spherical and PEG - MgO has 0D- spherical shape while that SDS- MgO has 1D-rod with hexagonal shapes with average crystalline sizes are ~20-80 nm and length of rods usually 200- 500 nm. The SAED patterns (inset of Fig. 2(a),(b),(c)) taken from individual crystallites showed clear rings corresponding to (200), (220) and (222) planes signifying that the synthesized particles are polycrystalline MgO with cubic structure.

The optical absorption spectra of SDS, PEG and CTAB-MgO nano powder were recorded to investigate their optical properties as shown in Fig. 3(a). The samples are in close to visible region and absorption maxima decreased which is minimization of crystallites and structural defects. The optical band gap was projected from the relation [9],

$$(\alpha h\nu)^2 = A(h\nu - E_g)^m \quad (4)$$

where α - absorption coefficient, A - constant, E_g - band gap energy, m - constant (for direct transition is 1). The linear fit of the curve extrapolated between $(\alpha h\nu)^2$ and photon energy axis ($h\nu$) gives

band gap energy shown in Fig. 3(b).

The obtained optical band gap is $E_g = 4.10\text{eV}$, 3.41eV and 3.12eV for SDS, PEG and CTAB-MgO nano powder respectively. The optical band gap has narrowed which is the electron transfer from valance band to conduction band easily. This consequence is well consistent with earlier reports [15, 16]. The absorption edge at higher wavelength region revealed that the nano powders can proficiently utilize for photocatalytic purpose.

CONCLUSION

In conclusion, we have produced three different surfactants roofed MgO nanopowder in nano dimensions by co-precipitation method. The XRD pattern revealed the Fm-3m space group with cubic phase and average crystallite sizes was about 33.75 nm, 20.27 nm and 18.70 nm for SDS, PEG and CTAB- MgO respectively. The small crystallites CTAB- MgO have a maximum strains were confirmed by Williamson Hall equation. The TEM pattern reveals 0D, 1D and 2D fine structure with less agglomeration and SAED pattern shows polycrystalline nature of the nano powders. The evaluated optical band gap energy is $E_g = 4.10\text{eV}$,

3.41eV and 3.12eV for SDS, PEG and CTAB-MgO nano powder respectively. The maximum absorption in near visible region signifying the possibility of utilizing these nano powders as an efficient photo catalyst and opto-electronic materials.

CONFLICT OF INTEREST

The authors declare that there are no conflicts of interest regarding the publication of this manuscript.

REFERENCE

1. Katsuro Hayashi, Satoru Matsuishi, Toshio Kamiya, Masahiro Hirano, Hideo Hosono. Light-induced conversion of an insulating refractory oxide into a persistent electronic conductor. *Nature* 2002; 419: 462- 465.
2. Jihyun Kim, Brent P. Gila, Rishabh Mehandru, J. Wayne Johnson, Ji- Yong Shin, Kyu-Pil Lee, Ben Luo, A. Onstine, Cammy R. Abernathy, Stephen J. Pearton, Fan Ren. Electrical characterization of GaN metal oxide semiconductor diodes using MgO as the gate oxide. *J. Electrochem. Soc.*, 2002; 149: G482.
3. Peidong Yang, Charles M. Lieber. Nanorod-superconductor composites: a pathway to materials with high critical current densities. *Science*, 1996; 273: 1836.
4. Gregory W. Peterson, Philip W. Bartram, Olga Koper, Kenneth J. Klabunde. Reactions of VX, GD, and HD with nanosize MgO. *J. Phys Chem B*, 1999; 103: 3225–3228.
5. Ilya V. Mishakov, Vladimir I. Zaikovskii, David S. Heroux, Alexander F. Bedilo, Vladimir V. Chesnokov, Alexander M. Volodin, Igor N. Martyanov, Svetlana V. Filimonova, Valentin N. Parmon, and Kenneth J. Klabunde. CF₂Cl₂ decomposition over nanocrystalline MgO: Evidence for long induction periods. *J. Phys Chem B*, 2005; 109: 6982–6989.
6. Lian YuanWang, Jichu Yang. Transesterification of soybean oil with nano-MgO or not in supercritical and subcritical methanol. *Fuel*, 2007; 86: 328–33.
7. X.Wang, W.Liu, H.Yang, X.Li, N.Li, R.Shi, H.Zhao, J.Yu. Low-temperature vapor–solid growth and excellent field emission performance of highly oriented SnO₂ nanorod arrays. *Acta Mater*, 2011; 59: 1291–1299.
8. T. Prozorova, G. Katabya, R. Prozorovb, A. Gedankenka. Effect of surfactant concentration on the size of coated ferromagnetic nanoparticles. *Thin Solid Films*, 1999; 340: 189-193.
9. N.M.A.Hadia, HusseinAbdel-HafezMohamed. Characteristics and optical properties of MgO nanowires synthesized by solvothermal method. *Mat. Sci. SemiCond. Prcss*, 2015; 29: 238- 244.
10. Ali Khorsand Zak, Abd. Majid Wan Haliza. M. Ebrahimizadeh Abrishami, Ramin Yousefi, X-ray analysis of ZnO nanoparticles by Williamson–Hall and size–strain plot methods. *Solid State Sci*, 2011; 13: 251-256.
11. T. Selvamani, A. Sinhamahapatra, D. Bhattacharjya, I. Mukhopadhyay. Rectangular MgO microsheets with strong catalytic activity. *Mat. Chem. Phys* 2011; 129: 853– 861.
12. Yongfen Zhang, Mingzhen Ma, Xinyu Zhang, Baoan Wang, Riping Liu, Synthesis, characterization, and catalytic property of nanosized MgO flakes with different shapes. *J. Alloys Comp* 2014; 590: 373–379.
13. J. Manikantana, H.B. Ramalingamb, B. Chandar Shekarc, B. Murugand, R. Ranjith Kumare, J. Sai Santhoshif. Wide bandgap of strontium doped Hafnium oxide nanoparticles for opto-electronic device applications- Synthesis and characterization. *Materials Letters* 2017; 186: 42–44.
14. Maria Dalores Guillen, Nerea Cabo. Characterization of edible oils and lard by Fourier transform infrared spectroscopy. Relationships between composition and frequency of concrete bands in the fingerprint region. *J. Am. Oil Chem. Soc.*, 1997; 74: 1281-1286.
15. HuihuWang, Seanghoon Baek, Jonghyuck Lee, Sangwoo Lim. High photocatalytic activity of silver-loaded ZnO-SnO₂ coupled catalysts. *Chem. Eng. J.*, 2009; 146: 355-361.
16. D. Q. Fang, Rosa Alejandra lukaszew, Thomas Frauenheim, Ruiquin Zhangn. Band gap engineering of GaN nanowires by surface functionalization. *Appl. Phys. Lett.* 2009; 94: 073116.